Applied Numerical Modeling in Geomechanics – 2020 – Billaux, Hazzard, Nelson & Schöpfer (eds.) Paper: 07-04

Microseismic structure evolution due to variation of liquid injection rate

Victor V. Nazimko[1], Ildar A. Saleev[2], Mykhailo O. Iliashov[2] & Ludmila M. Zakharova[1]
[1]*Department of Ground Control, Institute for Physics of Mining Processes NAS Ukraine, Dnipro, Ukraine*
[2]*CJSC "Donetsksteel" – iron and steel works, Pokrovs'k, Ukraine*

1 INTRODUCTION

Hydraulic fracturing process (HF) has become very popular during exploitation of hydrocarbon and hydro-thermal resources (Kozlowska et al. 2018). HF involves high-pressure fluid injection into geologic deep strata that creates cracks in the deep-rock formations to stimulate well production. The efficiency of HF depends on several geological and hydro-mechanical parameters, namely pore pressure, strata permeability and anisotropy, mechanical stress in the rock mass and its strength, as well as the rate of fluid injection (Segall & Lu 2015). The rock mass transmits pumped liquid and dissipates energy, transforming potential energy of rock mass and fluid into kinetic energy of dynamic deformation, which generates microseismic events during HF deployment. Since the rate of loading affects microseismicity (Guérin-Marthe et al. 2019), patterns of microseismic structure depend on the rate of injection and appear as micro- and macro-arrays of the seismic activity that diffuses in spatiotemporal system of coordinates (Hummel & Müller 2008). HF spreads irregularly in the rock mass disintegrating the weakest patches of the strata that causes strata to surrender a possible minimum of valuable energy resource. Therefore, evolution of microseismic structure should be controlled. Investigation of the injection rate effect on the microseismic structure evolution and optimization of HF parameters are the objects of this presentation.

2 DESIGN AND ANALYSIS

We applied *FLAC3D* (Itasca 2006), a commercial code that simulates propagation of perturbation from an unbalanced force as well as damping of equations of motion and dissipation of the kinetic energy in the rock mass. *FLAC3D* can simulate flow of injected liquid in parallel with the mechanical modeling, and thus capture the effects of fluid/solid interaction.

Those processes follow HF deployment and might reveal specific patterns of microseismic activity of fractured rock mass. According to Aki & Richards (2002) scalar seismic moment M is defined by the equation

$$M = G \cdot A \cdot D, \tag{1}$$

where G is the shear modulus of the rocks involved in the micro-earthquake; A is the area of the rupture along the fracture, produced by HF; D is the average of displacement between the two sides of the fracture.

We calculated M according to the next formula:

$$M = Mod \cdot V \cdot \Delta S, \tag{2}$$

where Mod is an average bulk modulus of the rock mass; V is volume of the fracture; ΔS is a strain increment (dimensionless) due to fracture emergence.

Traditionally, *M* having dimension [Nm] is considered as a moment. However, it may be reasoned as the work produced during development of an individual fracture or a fault. We may relate this work to a certain volume, in this case, to the volume of the zone where the fault has been developed. Therefore, we simplified formula (2), cutting the multiplier *V*.

Fracture initiation was simulated using the criterion proposed by Hubbert & Willis (1957):

$$Pb = 3\sigma h - \sigma H + T - Po \quad (3)$$

where *Pb* is breakdown pressure; σh and σH are minimum and maximum horizontal in-situ stresses, respectively; *T* is tensile strength of a rock layer, *Po* is the pore pressure. The orthotropic rock mass was assumed to be perfectly brittle in tension, and seismicity was associated with tensile cracking only. Young's moduli e1, e2, e3 and shear moduli g1, g2, and g3 (see Table 1) were corrected in the zones where current pore pressure reached to *Pb*. These moduli were diminished proportionally to corresponding normal and share strain increments.

Fracture generation increases permeability of the rock volume. Every component of permeability (for example k_y) increases due to increment of one normal strain (ssi_y) and two shear (ssi_{yx} and ssi_{zy}), which develop after the fracturing. We used the recommendation of Min et al. (2004) to correct the permeability:

$$k1' = k1\,(1 + fnorm\,(\Delta S1)^3 + ftan\,(\Delta S12 + \Delta S13)) \quad (4)$$

where *k1* and *k1'* are permeability along direction 1 before and after HF; $\Delta S1$ is the normal component of strain increment; $\Delta S12$ and $\Delta S13$ are tangential components of strain increments in planes 12 and 13; *fnorm* and *ftan* are empirical coefficients 0.83 and 0.095 respectively. The other components of anisotropic permeability *k2* and *k3* were recalculated with corresponding index permutation.

We simulated HF for a case of Ukrainian coal deposit 'Pokrovs'ke'. The thickness of the coal seam was 1.8 m. It absorbed up to 20 m^3 of methane per ton of coal. The model was divided into 9456 zones containing 12,829 grid nodes. Dimensions of the model were 300 m along horizontal axis X and Z. The top and bottom of the model were at 440 m and 288 m from the origin of coordinate system, respectively (Fig. 1). Mechanical and hydraulic properties of the strata are presented in Tables 1 and 2. The fractures were not simulated explicitly but have been accounted for through anisotropy of permeability. The liquid was injected under a constant rate. Three cases were investigated: for injection rate of 0.01, 0.06, and 0.12 m^3/s in the order given.

Table 1. Mechanical properties of the rock mass.

Young's modulus, Pa			Shear modulus, Pa			Poisson ratio			Tensile limit, MPa
e1	e2	e3	g1	g2	g3	nu1	nu2	nu3	T
$4\cdot10^8$	$4\cdot10^8$	$4\cdot10^8$	$1.6\cdot10^8$	$1.6\cdot10^8$	$1.6\cdot10^8$	0.25	0.25	0.25	$2\cdot10^5$

Table 2. Hydraulic properties.

Permeability, m/s			Pore pressure, Pa	Fluid bulk modulus, Pa	Porosity	Rate of liquid injection, m^3/s
$k1=k_y$	$k2=k_z$	$k3=k_x$	pp	fmod	Por	vwell
$2\cdot10^{-7}$	$4\cdot10^{-8}$	$2\cdot10^{-7}$	$2\cdot10^6$	$5\cdot10^7$	0.1	0.01; 0.06; 0.12

Displacements, which are normal to lateral walls of the model, were fixed. All components of displacements were restricted on the bottom. Depth of 800 m was simulated at the level of the liquid injection. Vertical and horizontal components of the geostatic stress σy, σx, and σz were 20, 10 and 10 MPa respectively at the point of injection.

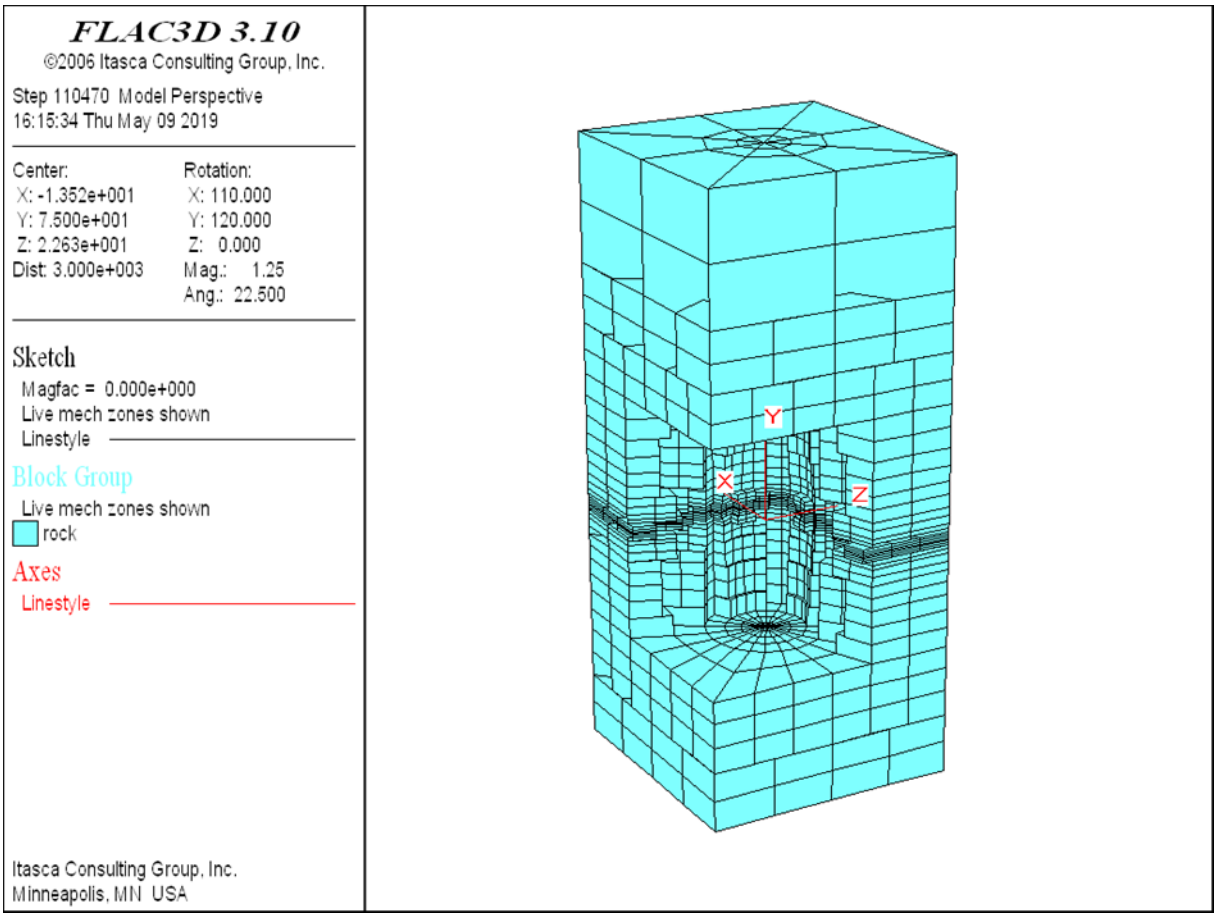

Figure 1. Model of the rock mass.

3 RESULTS AND DISCUSSION

Figure 2 depicts seismic moment distributions in the rock layer where liquid was injected. The interval Y = 0 ± 1 m encompasses a rock layer, which is the closest to the point of injection. First, the closer the layer to the point of injection the more intensive the microseismicity and the more vivid the picture of seismic structure is. Second, every rock layer provides its own distribution of the seismicity having individual peculiarities because there are the boundaries between the layers, which refract seismic waves and change their distributions essentially. Therefore, overlay of the distributions from several layers makes the integral distribution complex that hides the patterns of possible structures. This distribution presented in coordinate 'time – distance from the source of injection' that is frequently used by researchers who investigate seismicity (Segal & Lu 2015) and reason that evolution of this distribution reflects the process of pore pressure diffusion (Hummel & Müller 2008, Parotidis et al. 2005). Time was scaled to provide visibility of the distributions.

The liquid flow, passing through this system, dissipated potential energy of the deformed rock mass, transformed this energy to kinetic energy of seismic events, which manifested as arrays of seismic activities in space and time. Swarms of maximum seismicity moved away from the source during HF deployment as indicated by the white arrows. In addition, the swarms had a complex structure. They consisted of a macrostructure of hills' series 1 and micro-chains of ripples 2. The more the rate of injection, the bigger maximal size of the fractured body. The length of this body along X-axis was 11, 25, and 46 m for the rate of injection of 0.01, 0.06, and 0.12 m^3/sec in that order.

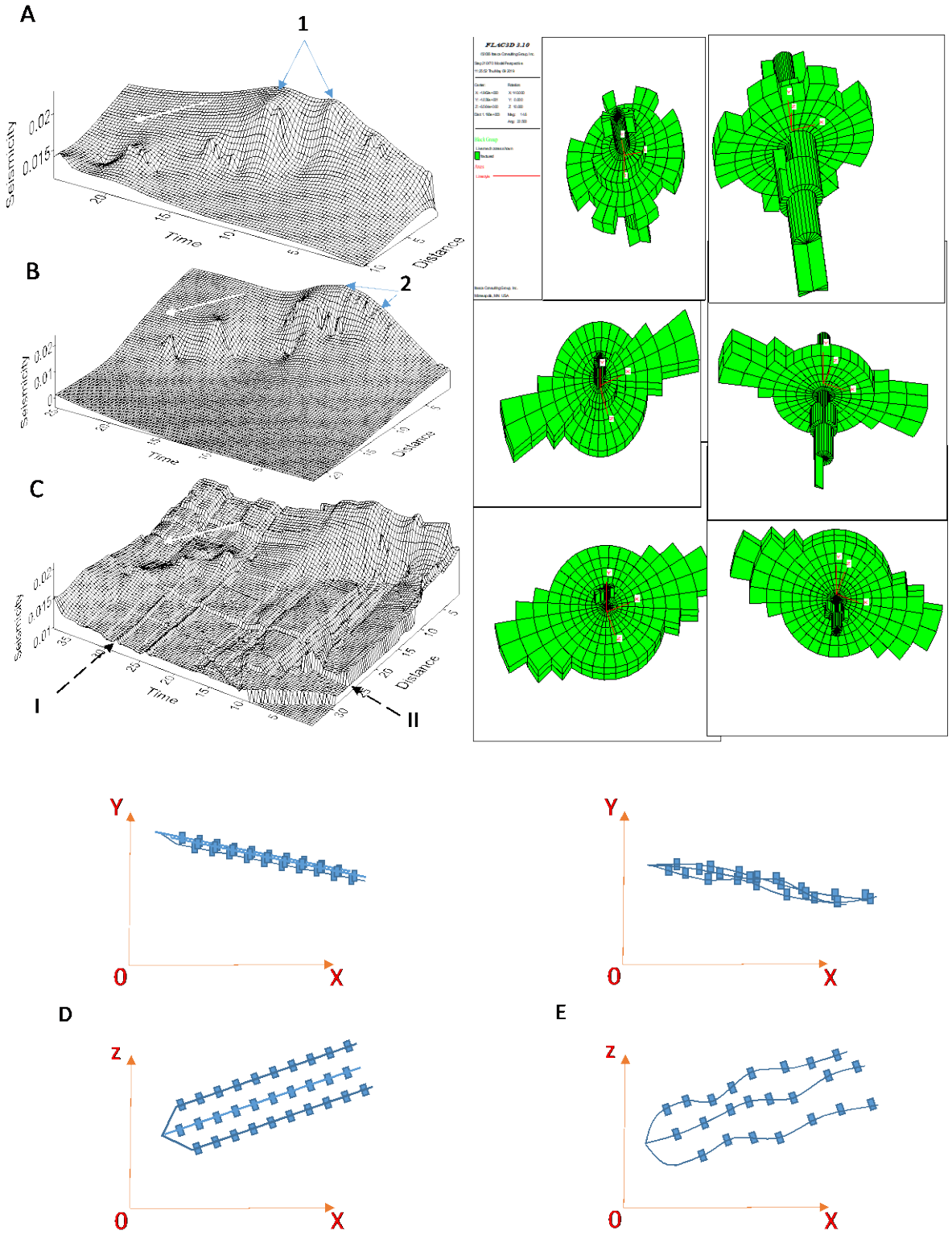

Figure 2. Spatio-temporal distribution of seismic activity in rock layer Y = 0 ± 1 m for the rate of injection of 0.01 m^3/s (A), 0.06 m^3/s (B), and 0.12 m^3/s (C); left and right green pictures show corresponding fractured bodies of the strata (top and bottom views); traditional layout of sub-horizontal wells (D), proposed arrangement of the wells and points of liquid injection (E).

The most intensive injection induced bifurcation creating extra sets of orthogonal structures I and II, which were approximately parallel to time and space coordinate axis (shown by intermitted arrows on Fig. 2c). Moderate rates of injection induced sequential fracturing that followed by serial hills of seismic activity. However, it seems that there is a critical rate of injection, which is more than 0.06 m^3/s for the case.

Arriving to this critical threshold, HF introduced another process, which triggered synchronous fragmentations of the strata to utilize extra energy flow (line I as an example). In addition, the HF process involved another mode of strata disintegration in the form of repeated seismic activation of the same fracture (line II) (Jin 2018). In other words, the rock mass involved new patterns of seismic dissipative structures (DS), which enabled absorbing and transforming of extra potential energy that was pumped into the strata by injected liquid with increasing rate. Such spontaneous process complies with self-organization principles in thermodynamics (Nicolis & Prigogine 1971) and was investigated in geomechanics (Nazimko & Zakharova 2017).

Our simulation demonstrated that a hydraulically fractured body expands asymmetrically in time and space relatively the source of liquid injection (green pictures in Fig. 2) even in the rock mass having uniform structure and continuous physical properties. The effect of sequential development of the fractured body is natural because it is physically expedient, namely such a specific order saves the energy and spends it more economically to produce the same amount of irreversible processes. Nicolis and Prigogine (1971) formulated such behavior as a minimum of excessive entropy production. *FLAC3D* numerically reproduced this behavior due to a general calculation sequence that invokes the equations of motion to derive new velocities and displacements from stresses and forces, which are calculated assuming the velocities are constant or 'frozen'. Such an assumption is physically viable if the time step is sufficiently small. It is impossible to overestimate significance of this calculation sequence for geomechanics because it allows DS reproducing and investigating a path of loading, which is unique during development of the irreversible processes.

Traditional technology uses an array of straight linear horizontal wells, and injection of liquid is conducted at a constant space interval (Kozlowska et al. 2018) as demonstrated schematically in Figure 2d. However, as our simulation showed, the seismic structures can induce anomalous distribution of microseismicity even in homogeneous uniform strata. There is no need for any discontinuity of physical properties in a rock layer in order to produce a certain seismic structure due to HF deployment. Nicolis & Prigogine (1971) showed that a slight fluctuation of temperature or pressure might trigger a self-organization of a DS in any thermodynamic system, which transmits sufficiently intensive flow of energy. In the case of the *FLAC3D* simulation, limited accuracy of calculation plays a role of the trigger and activates a certain pattern of DS. Thus, occurrence of the DS is unavoidable during HF even in the rock mass having uniform structure and continuous physical properties. Furthermore, any discontinuity will aggravate this process, and designers should consider certain measures to control DS. Natural variation of physical parameters and geologic structure will enlarge these anomalies, what makes more pronounced irregular hydrofracturing of gas bearing strata.

Therefore, the process of seismic diffusion should be controlled. HF parameters should account for the irregular dissemination of the induced fractures and adapt to the anomalies. Parameters of HF have to provide as consistent fracturing of the strata as possible. To do this, traces of the wells should deviate to go through the patches characterized with maximum strength and tightness of the rock mass. Furthermore, points of fluid injection ought to be set at centroids of those problematic patches (Fig. 2e). Preliminary assessment has shown that such measures could increase the yield of coalbed methane up to 1.5 times reducing the number of wells by 20%.

4 CONCLUSIONS

FLAC3D was used to simulate the evolution of the microseismic process due to variation of liquid injection rate during HF deployment in homogeneous uniformly layered coal bearing strata. HF process was followed by diffusion of microseismicity in a form of hills' arrays and ripples' sequences in space 'time of injection – distance from the source injection'. Maxima of seismic activity in hydraulically connected zones followed each other by turn, one after another This violated symmetric development of the fractured body in spite of the fact that the initial rock mass had geometric and physical symmetry relative to the point of liquid injection. In addition, patterns of microseismicity became more complex as the rate of liquid injection

increased. First, synchronous periodic triggering of seismic activity occurred through the entire fractured body, second repeated hydraulic fracturing emerged at certain distances from the source of injection. Investigation of the evolution of microseismic structure helped to propose practical measures, which can increase efficiency of HF. Evolution of induced seismicity should be controlled to provide as consistent fracturing of the strata as possible. The consistent fracturing may be accomplished if (1) horizontal wells deviate and go through the most competent and tight patches of the strata, and (2) the interval between adjacent points of injection are not constant and the points concentrate at the competent patches. Such approaches could increase the amount of the extracted coalbed methane up to 1.5 times and, at the same time, reduce the number of wells by 20%.

REFERENCES

Aki, K. & Richards, P.G. 2002. *Quantitative seismology* (2 ed.). Sausalito, California: University Science Books

Guérin-Marthe, S., Nielsen, S., Bird, R., Giani, S., & Toro, G.D. 2019. Earthquake Nucleation Size: Evidence of Loading Rate Dependence in Laboratory Faults. *Journal of Geophysical Research: Solid Earth* 124.

Hubbert, M. K. & Willis, D. G. 1957. Mechanics of hydraulic fracturing. *US Geological Survey* 210: 153-168.

Hummel, N. & Müller, T.M. 2008. Microseismic signatures of nonlinear pore pressure diffusion. *SEG Technical Program Expanded Abstracts*, 1382-1386.

Itasca Consulting Group, Inc. 2006. *FLAC3D – Fast Lagrangian Analysis of Continua in 3-Dimensions, Ver. 3.1*. Minneapolis: Itasca.

Jin, L. 2018. Hydromechanical-Stochastic Modeling of Fluid-Induced Seismicity in Fractured Poroelastic Media. *EarthArXiv*.

Kozlowska, M. et al. 2018. Maturity of nearby faults influences seismic hazard from hydraulic fracturing. *PNAS*. February 20, 2018 115 (8) E1720-E1729. https://doi/10.1073/pnas.1715284115

Min, K-B., Rutqvist, J., Tsang, C-F. & Jing, L. 2004. Stress-dependent permeability of fractured rock masses: a numerical study. *International Journal of Rock Mechanics and Mining Sciences* 41(7): 1191–1210.

Nazimko, V.V. & Zakharova, L.M. 2017. Cluster behavior of the ground during its irreversible movement. *Acta geodynamica et geomaterialia* 14(188): 45-49. 10.13168/AGG.2017.0025.

Nicolis, G. & Prigogine, I. 1971. *Self-Organization in Nonequilibrium Systems: From Dissipative Structures to Order through Fluctuations*. New York: Wiley.

Parotidis, M., Shapiro, S. A. & Rothert, E. 2005. Evidence for triggering of the Vogtland swarms 2000 by pore pressure diffusion, *J. Geophys. Res.*, 110, B05S10, doi:10.1029/2004JB003267.

Segall, P. & Lu, S. 2015. Injection-induced seismicity: Poroelastic and earthquake nucleation effects. *J. Geophys. Res. Solid Earth* 120: 5082–5103.